Modification of Electronic Properties of Mo_2C Catalyst by Potassium Doping: Impact on the Reactivity in Hydrodenitrogenation Reaction of Indole

Andrzej Kotarba,*,† Grzegorz Adamski,†,§ Witold Piskorz,† Zbigniew Sojka,†,‡ Celine Sayag,§ and Gérald Djéga-Mariadassou§

Faculty of Chemistry, Jagiellonian University, Ingardena 3, 30-060 Cracow, Poland, Regional Laboratory of Physicochemical Analyses and Structural Research, Ingardena 3, 30-060 Cracow, Poland, and Université Pierre et Marie Curie, Laboratoire Réactivité de Surface, UMR CNRS 7609, 4, Place Jussieu, Case 178, 75252 Paris Cedex 05, France

Received: October 14, 2003; In Final Form: December 29, 2003

The effect of potassium doping on electronic surface properties of molybdenum carbide (Mo_2C) was investigated by species-resolved thermal alkali desorption techniques, work-function measurements, and density-functional theory calculations. The activation energies for desorption of K and K^+ were determined and used for work-function assessment via the Schottky cycle. The results were compared with the parallel contact potential difference measurements, and a variation of the Fermi level upon doping was rationalized in terms of the potassium coverage and surface dipole moment. The tight correlation between the work-function changes and the rate constant of indole hydrodenitrogenation was observed and discussed in terms of electrophobic promotion.

1. Introduction

The molybdenum carbide (Mo_2C) exhibits catalytic properties similar to those of noble metals and might be used as a cheaper substitute for catalysts of deep hydrodesulfurization and hydrodenitrogenation (HDN) processes,[1,2,3] which are becoming of vital importance for petroleum processing. Among organonitrogen compounds from petroleum or coal-derived feedstock, indole is one of the most common molecules used for probing the catalytic HDN performance. The reaction was thoroughly investigated and some general consensus concerning its kinetics and mechanism has been achieved.

Because of the lattice expansion, insertion of carbon atoms into the lattice of molybdenum leads to the appearance of a narrower metallic-type band with the density of states at the Fermi level similar to that of noble metals.[4] Oxygen can also be incorporated into the lattice of Mo_2C, giving rise to the appearance of acidic properties. As a result, the surfaces of such materials can behave as bifunctional catalysts, and the balance between metallic and acidic properties strongly depends on their actual chemical state.[5,6]

A simple tool for modifying the surface properties of catalytic materials widely exploited in heterogeneous catalysis consists of alkali doping.[7,8,9] The introduction of alkali ions generates electrostatic fields of the order of tens V/nm at the surface,[9] inducing substantial changes in the course of adsorption and catalytic reactions. Various explanations have been proposed to rationalize the alkali promotion effects. They involved a direct overlapping of the adsorbate and alkali ion wave functions, a change in the position of the donor−acceptor energy levels of adsorbed molecules, and short- or long-range electrostatic interactions. Some of these issues have been discussed and exemplified by Somorjai, Bonzel, Schlögl,[8,9] Pacchioni et al.[10] and more recently by Vayenas in the field of electrocatalysis.[11]

Owing to the exceptionally low ionization potentials of alkali metals, a substantial part of the promotion effect is thought to be related to the charge transfer to the catalyst surface, inducing an electric field gradient at the surface, generated by the resulting dipole and modification of the density of states characteristics. Such effects are specially pronounced in the case of heavy alkali atoms because their large ionic radii give rise to large values of the dipole moment ($\mu_s \approx 5-10$ D) and the associated work function changes ($\Delta\Phi \propto n\Delta\mu_s$).[12] Obviously, the addition of alkali will influence also the acid−base properties of the catalyst surface, especially at high loadings.

The idea of prime importance of the Fermi-level electrons and the associated density of states is not new in catalysis.[13,14] In the frontier orbital picture of bonding to surfaces, the states near the Fermi level play the role of HOMO and LUMO in molecular interactions since their electrons can be rearranged at the least energetic expenses.[15] Thus, the E_F/DOS parameters have a useful, predictive value for the electrophilic or electrophobic activation of the incoming reactants.[16] The unique electron properties of alkali adatoms can be utilized to shift the position of the Fermi level of the catalyst. Then, by looking at the response of the reaction rate to the change in concentration of an alkali promoter, we can distinguish between those pathways that are favored by enhancement or depletion of the electron density in the kinetically significant surface species. An elegant demonstration of the relevance of those functionalities can be provided, e.g., by calculations of the change in electronic properties of single Rh(001) crystal surface after Li, Cl, P, or S adsorption.[17] An analogous approach has been used to account for the potassium promotion in activation of N_2 on the surface of a fused iron catalyst for the industrial ammonia synthesis.[18]

* Author to whom correspondence may be addressed. Fax: +48 12 6340515. E-mail: kotarba@chemia.uj.edu.pl.

† Jagiellonian University.

‡ Regional Laboratory of Physicochemical Analyses and Structural Research.

§ Université Pierre et Marie Curie.

10.1021/jp037105j CCC: $27.50
Published on Web 02/04/2004

Taking into account the abovementioned considerations, it is not surprising that the most pronounced electronic promotion has been found in the case of K, Rb, and Cs. For practical reasons, since potassium is least expensive, it is naturally the most widely used element in the industrial heterogeneous catalysis. Ammonia synthesis, Fischer−Tropsch hydrocarbon synthesis, or dehydrogenation of ethylbenzene to styrene are well-known examples where the promotion with the potassium is one of the critical aspects in ascertaining a good catalytic performance.[7−9]

In this paper, we focused our attention on the modification of the electronic properties of Mo_2C as a function of K loading and the source of the promoter (KOH dissolved in 2-propanol or K-naphthanele complex dissolved in THF). The experimentally determined work-function changes upon K doping are complemented with the density-functional theory (DFT) calculations of density of states structure and the position of the Fermi level, using the cluster approach. The impact of K doping on the kinetics of the HDN reaction of indole was quantified and correlated with the catalyst work function.

2. Experimental and Methods

2.1. Materials. The detailed description of the preparation procedure of the molybdenum carbide can be found elsewhere.[19,20] Shortly, the Mo_2C catalysts were prepared by temperature-programmed carburization of the MoO_3 precursor. The reaction was carried out under the atmospheric pressure in a flow of CH_4/H_2 gas mixture (10 vol %) with the gas hourly space velocity = 68 h^{-1}. The temperature was linearly increased at the rate of 53 K h^{-1}, from room temperature to 1023 K, where it was maintained for 1 h. Then the samples were quenched to room temperature in a flow of helium and gradually passivated with 0.5-cm^3 pulses of O_2 until complete saturation of the surface.

Alkali addition can be effected in two main ways: through *nascent-doping*, when the promoter is added to the oxide precursor before the carburization reaction, and through *post-doping*, when it is added after the synthesis of the final carbide. The first procedure was found to inhibit significantly the carburization process driving the synthesis toward the metallic molybdenum,[21] and additionally in such a case, only a part of the promoter was presented at the external surface. Therefore, in this study, the potassium promotion was accomplished by the *post-doping* procedure from 0.2 M solution of KOH in 2-propanol or using a 1:1 K−naphthalene charge-transfer complex dissolved in THF. The samples were doped with 0.002, 0.01, 0.05, 0.2, and 1 wt % of potassium, which corresponds to a surface coverage (Θ_K) ranging from 10^{-3} to 10^{-1} of the monolayer (ML). For the thermal K-desorption experiments, all samples were pressed to form tablets of 10 mm in diameter and typical mass of 100 mg.

The samples were characterized by X-ray diffraction analysis (XRD), scanning electron microscopy (SEM), transmission electron microscopy (TEM), BET surface area measurements, and CO-chemisorption methods. The X-ray measurements were performed with Cu Kα monochromatized radiation using a Siemens D500 automatic powder diffractometer. The morphology of the samples was examined with a JEOL-JEM 100 CXII transmission microscope operating at 100 kV and associated with a top entry device. The powder was dispersed ultrasonically in xylene and deposited on a copper grid, previously coated with a carbon film. The specific surface area of the samples was determined in a flow regime by means of N_2 adsorption. The measurements were performed using a Quantachrome instrument. For CO-chemisorption measurements, pulses of 20 μmol of CO (Air Liquide 99.997%) in flowing He (Air Liquide 99.995%) were injected on the sample every 2 min. The procedure was continued until the surface was completely saturated with the CO molecules and the amount of chemisorbed CO was measured by TCD. Prior to the CO-chemisorption measurements, after the synthesis, the samples were passivated, then the potassium was added and the promoted samples were rejuvenated by repeating the synthesis procedure (vide supra). The results are summarized in Table 1.

TABLE 1: Characterization of K-Doped Mo_2C Catalysts

K content (wt %)	surface coverage (ML)	CO uptake (μmol × g^{-1})	k_{IND} (s^{-1})
0.0	0	270	50.6 ± 2.9
0.002	6×10^{-4}	240	
0.01	3×10^{-3}	210	29.6 ± 2.2
0.05	1.5×10^{-2}	215	
0.2	6×10^{-2}	210	44.4 ± 3.3
1.0	3×10^{-1}	200	14.8 ± 1.2

2.2. Techniques. For characterization of the potassium promoter on the Mo_2C surface, the recently developed species-resolved (detection of atoms, ions, and excited states) thermal alkali desorption method (SR-TAD) was used.[22] The desorption experiments were carried out in a vacuum apparatus with a background pressure of 10^{-7} mbar. The samples were heated from room temperature to 850 K in the intermittent mode with the heating rate of 5 K min^{-1}. The ions leaving the catalyst surface under these conditions are K^+, as revealed by quadrupole mass spectrometry screening. Since the sample was held at a positive potential of 100 V, practically all potassium ions formed on the surface were accelerated toward the collector. The flux of K atoms was measured by a surface ionization detector,[23] whereas that of K^+ was monitored directly as an ionic current of the collector in a field ionization detector.[24]

The contact potential difference (CPD) measurements were carried out by the dynamic condenser method of Kelvin with a KP-6500 probe (McAllister Technical Services). The reference electrode was a stainless steel plate with a diameter of 10 mm. During the measurements, the gradient of the peak-to-peak vs backing potential was set to 1, whereas the vibration frequency was equal to 120 Hz. The CPD was calculated from 8 experimental points, each being an average of 20 measurements.

For DFT computations, the Mo_2C was modeled with the $Mo_{24}C_6$ cluster. The cluster was cut off from the hexagonal Mo_2C crystal (*P*6*m*2 structure) taken from the database of Cerius[2] (Accelrys). The calculations were performed within the Kohn−Sham formalism implemented in the DMol-960 program (InsightII release 95.0, Biosym/MSI, San Diego, 1995) using local density approximation with the VWN correlation-exchange potential[25] and DNP basis set (double numerical augmented by polarization functions). Such an approach has been successfully used for the calculations of the band and the density of states (DOS) structures for the number of solids, such as transition-metal oxides,[26] sulfides,[27] and carbides,[28] and it has been found that the replacement of LDA by gradient-corrected GGA functionals gave essentially the same results.

The geometry of clusters was fully optimized using numerical gradients and the BFGS (Broyden−Fletcher−Goldfarb−Shanno) method.[29] The SCF electron density convergence criterion was set at 10^{-6} au. The optimization was based on the gradient displacement norms (10^{-3} au.) and threshold for energy set at 10^{-5} au. In the case of the K-promoted Mo_2C, a potassium atom was placed either on the surface (above the central Mo atom) or embedded into the framework of the cluster (in the

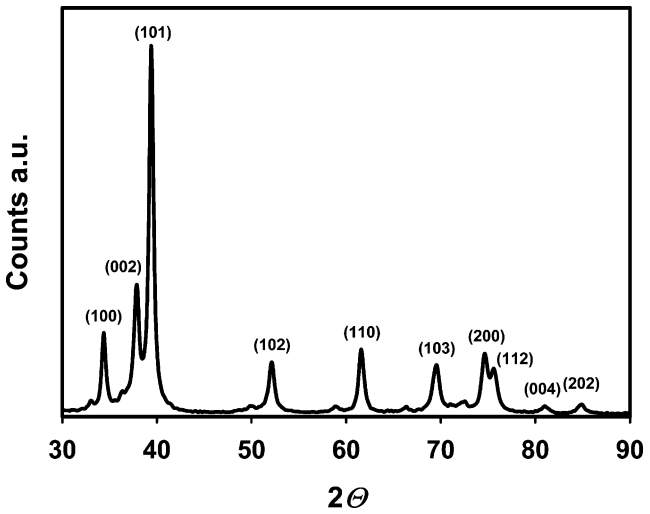

Figure 1. XRD pattern of the synthesized β-Mo_2C catalyst indexed in *P*63/*mmc* space group (JCPDS 35-0787).

cavity formed by Mo atoms) and the geometry was fully reoptimized. The latter situation corresponding to the *nascent-doping* gave the potassium desorption energies five times higher than those observed in thermal desorption experiments, so it was not taken into account in further modeling.

The catalytic tests of indole hydrodenitrogenation were performed in a dynamic high-pressure flow reactor equipped with a piston pump (Gilson 302), injecting the indole/cyclohexane/decane (reactant/solvent/internal standard) mixture into the hydrogen carrier gas (Air Liquide, 99.995%). Indole, cyclohexane, and decane with a grade of 99+% were purchased from Acros Organics. The pressure in the catalytic unit was regulated using a backpressure valve (Brooks 5866), and the gas flow rate was controlled by mass flow controllers (Brooks 5850 TR). Reactants and products were separated and analyzed online on an ultra 1 methyl silicone gum capillary column (50-m long and 0.33-μm of the internal diameter) installed in a Hewlett-Packard GC 5890 gas chromatograph equipped with an ionization flame detector. The measurements were carried out at 573 K, under the pressure of 50 atm, the contact time varying from 0.03 to 0.7 s and the hydrocarbon to hydrogen volumetric ratio of 1/1000. Prior to the catalytic tests, the catalysts were activated in pure hydrogen at 723 K for 2 h. At the test conditions, no appreciable deactivation of the catalysts was observed for at least two weeks of time-on-stream. The kinetic results (conversion vs contact time) were analyzed in terms of the two coupled pathways[30,31] of early (EDN) and late (LDN) denitrogenation reactions.

3. Results and Discussion

3.1. Catalyst Characterization. The phase identity of the catalysts was confirmed by XRD measurements using the JCPDS 35-0787 database as the reference. In all the synthesized samples, only the diffraction pattern characteristic of the β-Mo_2C hexagonal compact phase was observed and the diffraction peaks can be readily indexed within the *P*63/*mmc* space group (Figure 1). The relative intensity ratios of the peaks agreed well with those of the standard powder diffraction file, indicating that the Mo_2C crystallites have random morphology without any pronounced preferential orientation. The morphology and particle size distribution of the molybdenum carbide was examined with the transmission electron microscope. A typical grain of the unpromoted catalyst along with the selected area diffraction pattern is shown in Figure 2. TEM micrographs showed a

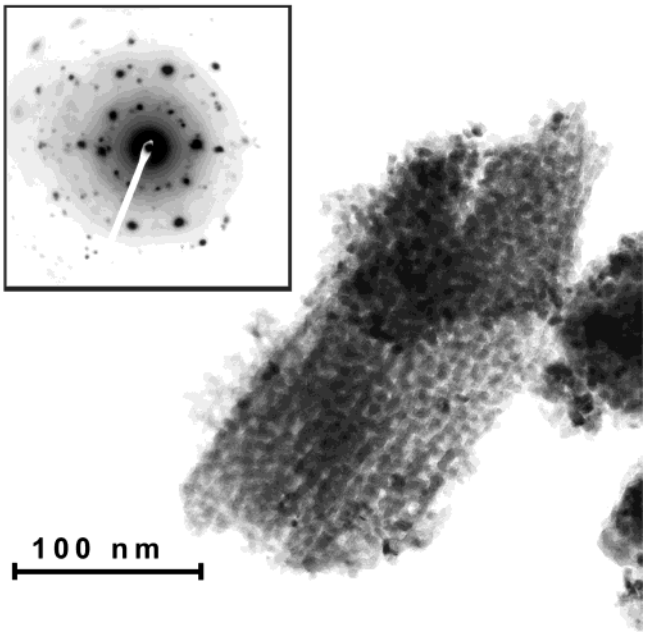

Figure 2. TEM micrograph of the typical grain of Mo_2C catalyst and the corresponding electron microdiffraction pattern in the insert.

uniform morphology of the samples with the average grain size of 10−20 nm. The grains were composed of loosely aggregated small rounded crystallites of the average diameter equal to 17 nm, derived from the X-ray line broadening using the Debye−Scherrer formula. For some crystallites, selected area electron diffraction was performed, confirming that the crystallites forming the catalyst grains are due to Mo_2C indeed. However, for some grains, small amounts of carbon deposit was also observed as well as traces of the MoC and Mo_4C_3 near kin phases. It is worth noting that the addition of potassium, even at low loadings before the carburization, resulted in a dramatic increase in the carbon deposit formation, supporting the advantage of the *post-doping* procedure.

The BET surface area (S_g) of the investigated samples was in the range of 50 ± 10 m^2 g^{-1}. Assuming the spherical shape of the crystallites, their average size d was calculated from the formula $d = 6/(\rho S_g)$, where ρ is the density of solid. The substitution of the numerical values to this equation yields $d = 14 \pm 3$ nm, which corresponds well to the results inferred from the X-ray line broadening.

The carbon monoxide is commonly used as a molecular probe to count metallic sites. Following the previous studies,[17,32] we assumed that the CO chemisorption is a nondissociative process with a 1:1 CO−Mo stoichiometry. The amount of the carbon monoxide chemisorbed was used to determine the number of the accessible surface molybdenum atoms, constituting the metallic active sites of the bare and K-doped Mo_2C catalysts. Taking into account that one CO molecule titrates one metallic site and assuming the theoretical number of exposed Mo atoms in hcp β-Mo_2C, from the data collected in Table 1, it can be inferred that only 25−40% of the total surface Mo atoms were accessible for the adsorption. The remaining part was blocked by the carbon deposits, clearly seen in TEM pictures, or harmed by the residual surface oxygen, which cannot be totally eliminated from the surfaces of transition-metal carbides.[17] The addition of potassium caused a distinct monotonic decrease in the number of surface metallic sites as indicated by the lowering of CO uptake (Table 1).

3.2. Potassium Desorption and Work Function. Isothermal potassium desorption curves showed clear first-order decay with

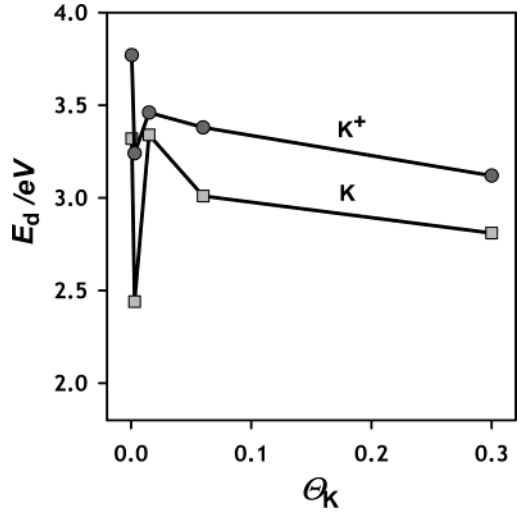

Figure 3. Effect of potassium surface coverage Θ_K on K and K^+ desorption energies. Potassium was deposited on the Mo_2C surface from (a) KOH/2-propanol and (b) K/THF solutions.

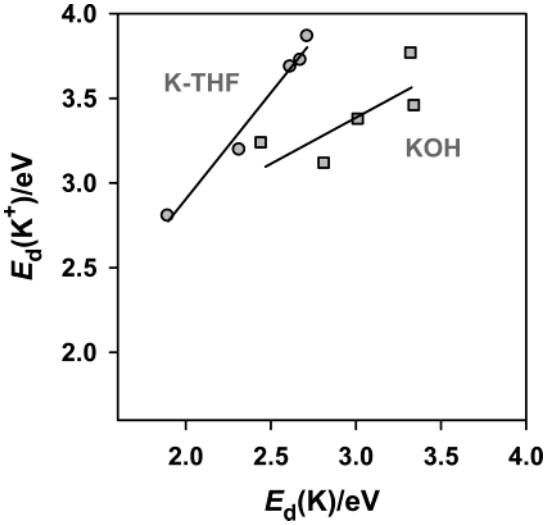

Figure 4. Desorption energies of potassium ions $E_d(K^+)$ and atoms $E_d(K)$ plotted against each other, showing the difference in stability and electron promotion, depending on the way potassium was deposited on the Mo_2C surface.

the rate constant depending on the potassium loading. In the measured temperature range, they varied from $2.2-6.5 \times 10^{-3}$ s^{-1}. The corresponding Arrhenius-like plots (logarithm of measured signals vs T^{-1}) were linear, and the correlation coefficients higher than 0.995 allowed the activation energies for the desorption of potassium atoms $E(K)$ and ions $E(K^+)$ to be determined with an error lower than 0.05 eV. This simple procedure for alkali metal desorption has been validated on various surfaces[33,23,24]. The values for K and K^+ desorption energy from the surface of Mo_2C as a function of surface coverage Θ_K are presented in Figure 3.

The stability of the K promoter on the Mo_2C surface strongly depended on the source and the level of doping. Two regions of surface coverage with distinctly different character of the changes in desorption energies can be distinguished. At low coverage ($0-0.05$), desorption energies were strongly dependent on Θ_K, whereas for the high coverage (> 0.05), the dependence was rather weak. An interesting feature, more clearly manifested in the case of doping from K/THF solution, was an unusual increase in K stability with Θ_K. Because of the repulsive interaction between the surface species, the desorption energy is normally expected to decrease with the coverage. There are only few systems described in the literature, NbC[34] and MoS_2,[35] where an increase in the potassium desorption energy with Θ_K was observed. The surface-clustering model is usually invoked to explain such finding. For the surfaces that are not wetted by the promoter, as the surface coverage increases, the mean cluster size becomes larger and the desorption energy augments. Following Volmer,[36] this phenomenon can be assigned to the cluster size dependence of the alkali vapor pressure. Smaller clusters, which exhibit higher vapor pressure, evaporate more quickly than the larger ones for which such pressure is lower, as it may be inferred from the Kelvin equation.

In Figure 4 the potassium stability diagram reveals the ranges of desorption energies observed for both K sources. Generally, the desorption energies for ions are higher than for atoms, indicating that the work function of the surface is smaller than the ionization potential I_K of potassium (vide infra). Indeed, the reported work function for Mo_2C is 3.85,[37] whereas $I_K = 4.34$ eV. The difference of the two procedures of doping consists mainly in the enhanced stabilization of K atoms in the case of doping from KOH/2-propanol solution. Since the desorption energies for K^+ are similar in both cases, the higher atomic stability of potassium *ex* KOH/2-propanol is linked with the lower electron promotion effect.

The molybdenum carbide is a conducting material with the conductivity approaching that of metals,[38] thus the Fermi level can be regarded as being uniform within the grains of the sample. By use of the values of desorption energies for K atoms ($E_d(K)$) and ions ($E_d(K^+)$), the work function Φ can be calculated from the Schottky cycle[39]

$$\Phi = E_d(K) - E_d(K^+) + I_K$$

The work function data are presented in parts a and b of Figure 5. Again for both of the measured series, independent of the source of potassium, a stronger effect was detected for low coverage. The Φ values for samples promoted with KOH/2-propanol are higher of about 0.5 eV than for the K/THF series implying that electronic promotion was more effective in the second case. The work function assessed from desorption data were next compared with the contact potential difference measured with the Kelvin Probe. As shown in Figure 5, the observed CPD exhibited very similar characteristics, proving the validity of the Schottky cycle for determination of the work function changes with K promotion in the case of the investigated solids.

Following the previous work, the charge perturbations due to alkali adsorption are screened over a short distance, whereas their effect on the DOS at the Fermi energy is observed at large distances, even at low coverage.[13] This suggests that to characterize the electronic properties of metallic surfaces (including carbides, nitrides, or metallic oxides), no matter whether ordered or disordered, clean or with adatoms, one should start by considering the DOS structure. In this way, the very important local aspects of catalytic surface processes can be unraveled in simultaneous accordance with the delocalized character of electrons in the metallic solid.

3.3. Insight into the Electronic Properties of Mo_2C from DFT Modeling. The structure of the $Mo_{24}C_6$ cluster with the potassium adatom optimized at the VWN level under the C_s symmetry is shown in Figure 6. It models the adsorption of K on the [0001] face of the Mo_2C crystal represented by two stacked layers, each composed of two edge-sharing molybdenum rings. The positions of Mo atoms in both layers are mutually

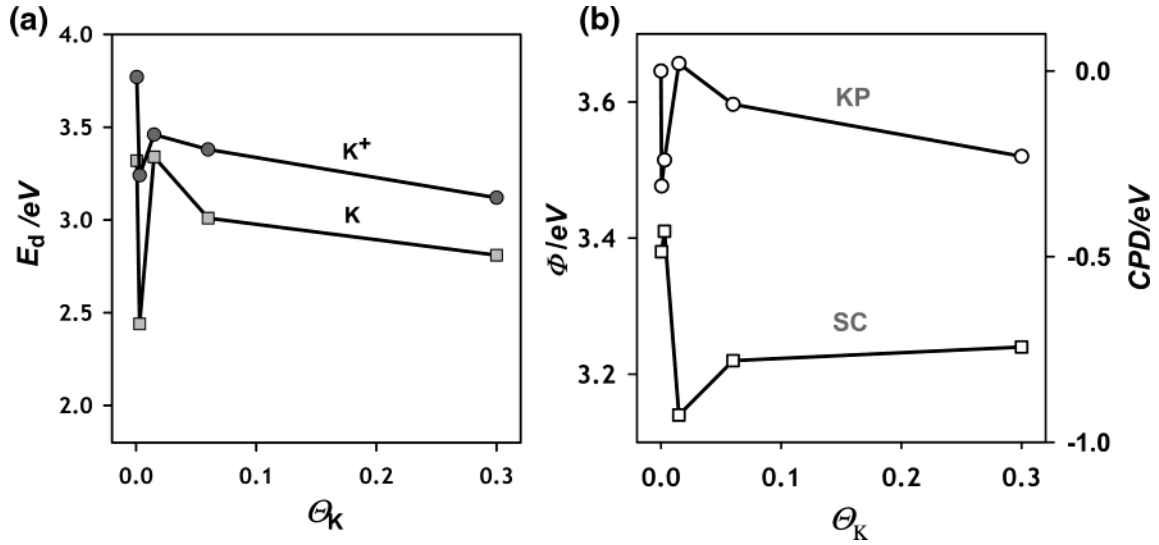

Figure 5. Effect of potassium surface coverage Θ_K on electronic properties of the K−Mo_2C catalyst. Work-function values were estimated from the Schottky energy cycle, whereas CPD was determined from Kelvin Probe measurement. Potassium was introduced on Mo_2C surface from (a) KOH/2-propanol and (b) K/THF solutions.

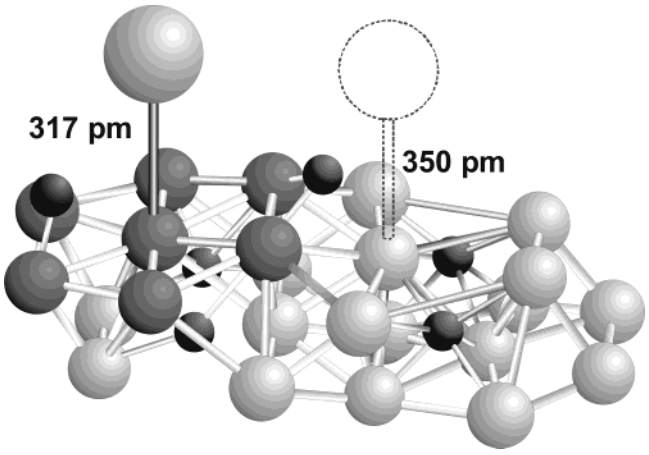

Figure 6. The optimized geometry of the $Mo_{24}C_6$ cluster with the potassium adatom. The alternative less-stable position is drawn with a dotted line. The polarized surface Mo atoms are marked by shadowing.

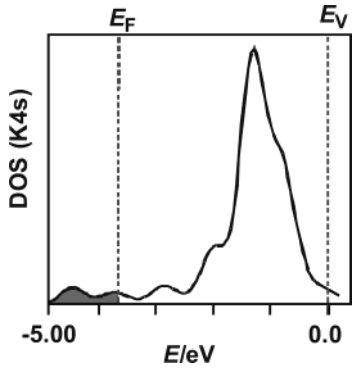

Figure 7. Density of states for the 4s orbital of the adsorbed potassium atom on $Mo_{24}C_6$ (E_F and E_V denote the energy of the Fermi and vacuum levels, respectively).

shifted by $^1/_2$ according to ABAB... stacking in the hcp structure of Mo_2C. The average Mo−Mo bond length was equal to 275 ± 2 pm for central atoms, whereas for peripheral atoms, it ranges from 248 to 337 pm for the most exposed ones. The ∠(Mo−Mo−Mo) angles (61.4−64.2°) were close to those in the ideal hexagon, showing a slight out-of-the-plane deformation. Indeed the two-dimensional regression gave the mean root mean square of the deviation of atomic positions with respect to the plane of the ring to be 6 pm only. The carbon atoms fill octahedral interstitials formed by closed packing of Mo atoms with the molybdenum−carbon bond distance $\langle d_{Mo-C}\rangle = 194 \pm 2$ pm and the ∠(Mo−C−Mo) angles in the range of 76−126° (with the average value close to 90°). The symmetry plane passes through the centers of all molybdenum rings.

To find its equilibrium position, the potassium atom was placed at the symmetry plane above the common edge of the Mo rings (Figure 6) on the upper layer and the geometry of the complex was reoptimized. The results revealed that the K atom was shifted toward the middle of the ring with the distance of 317 pm above the central Mo atom. Above the hexagonal ring another equilibrium position of the potassium was also found (shown by a dot line in Figure 6) at the K−Mo distance equal to 350 pm, but having a distinctly higher energy, this adsorption mode was not taken into account. The potassium adatom caused some relaxation of the geometry of the nearest molybdenum atoms, but the perturbation of the bond lengths was, however, smaller than 10 pm. More important were the significant changes in the Hirshfeld charges at the adjacent Mo atoms (marked darker in Figure 6), indicating distinct accumulation of the electron density in the vicinity of potassium, which counterbalances its positive charge ($q_K = 0.457$). Thus, the electron density released by potassium is transferred not to the entire cluster but it concentrates preferentially (87%) near the K adatom. Such a situation can be rationalized in terms of a surface dipole model. The dipole moment approximated from the classic formula $\mu_{surf} = 2q_K d_{K-Mo}$[40] was found to be 5.8 D, which is a typical value for the potassium on various surfaces of transition metals[41] and oxides.[42]

Additional information on the change in electronic properties in the presence of potassium on the $Mo_{24}C_6$ cluster can be inferred from the density of states (see Figures 7 and 8). For the clarity of further discussion, the DOS was divided into three main energy regions ($-12.5 < E < -9.5$; $-6.5 < E < E_F = 0$; $E > E_F$). In region I, the DOS structure is dominated by carbon s (35%) hydbridized with molybdenum d (65%) orbitals. The main maxima in this region were located at −11.5 and −10 eV below the Fermi level. The valence region II separated from region I by a gap of 2.5 eV contains strongly hybridized C p and Mo d electronic states. The main maxima appeared at −5.5

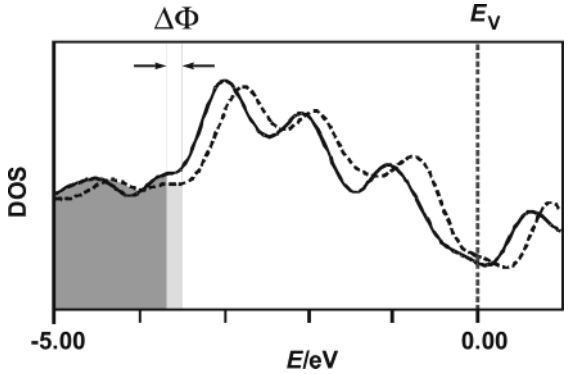

Figure 8. Change in the density of states of $Mo_{24}C_6$ (solid line) due to adsorption of K (dashed line). Energies are given with respect to the vacuum level (E_v). The change in work function ($\Delta\Phi$) due to Fermi-level shift of 0.2 eV is indicated.

eV (composed of 50% C p and 50% Mo d) and −2.4 eV (16% C p and 84% Mo d). The electronic states around the Fermi level were mainly due to Mo d with a 24% contribution from C p, while in region III, four maxima (for $E < 5$ eV) could be distinguished at 0.8, 1.6, 2.8, and 4.4 eV composed mainly of Mo d (73, 76, 64, and 63% respectively) hybridized with C p. These bands run continuously through the Fermi level, accounting for the metallic properties of Mo_2C. The obtained DOS structure for Mo_2C was in a good accordance with the results of more accurate calculations, using the full potential linear muffin-tin orbital method within the LDA approximation and the Hedin−Lundquist parametrization for the exchange correlation.[43]

The addition of potassium to the $Mo_{24}C_6$ cluster had feeble and rather uniform influence on the DOS below E_F. The major feature appeared at 2.5 eV above E_F (due to the 4s orbital of potassium) (Figure 7). Thus, upon adsorption, this orbital initially occupied by an electron was emptied, implying that the potassium adatom was present in the form of $K^{\delta+}$ ion in accordance with the experimental results of work-function measurements (vide supra). The resultant positive ion of potassium is screened by the electrons inside the cluster (note the polarized Mo atoms in Figure 6), producing the already brought up dipole with the positive end directed outward. This counterbalances the surface contribution to the work function of the Mo_2C.[41]

In Figure 8, the total DOS around the Fermi level for the $Mo_{24}C_6$ cluster with and without the K adatom are compared. The zero of the energy scale was set at the vacuum level (E_v). The Fermi energy (E_F) of bare and K-doped clusters equal to −3.53 and −3.73 eV, respectively, indicates the lowering in the work function by 0.2 eV upon K doping. This remains in very good agreement with the experimentally determined shift of the work function by two independent methods (contact potential measurements and from potassium desorption data via the Schottky cycle).

The compatibility of the theoretical and experimental data can further be reinforced by the analysis of the surface dipole formed by the potassium adatom. Generally, the work function Φ can be directly related to the coverage Θ_i of the promoting species via the Helmholtz formula[10]

$$\Delta\Phi = \frac{ne}{\epsilon_0}\sum_i \mu_i \Delta\Theta_i$$

where μ_i is the surface dipole (which generally is a coverage-dependent quantity), n denotes the number of adspecies, and ϵ_0 vacuum permittivity. The summation extends over all the adsorbed species. In the case of a single promoter, assuming that within the investigated coverage range μ_i remains nearly constant, this formula reduces to a simple relationship[44]

$$\Delta\Phi = ne\mu_S/\epsilon_0$$

Thus, for theoretically calculated decrease in the work function of 0.2 eV and $\mu_S = 5.6$ D, we can assess the associated number of K atoms per cm^2 $n = 10^{13}$, which corresponds to the coverage of $\Theta_K \approx 0.003$. Both these values nicely matched the highest experimentally determined work function shift $\Delta\Phi = 0.2$ eV, observed at the coverage Θ_K in the range of 0.001−0.002.

Since the work function sharply responds to the potassium doping and can be assessed by several independent methods, it is a convenient concise index to follow the changes in electronic structure in relation to surface reactivity according to the electronic theory of catalysis.[45,46]

3.4. Impact of Work Function on the Rate of Indole Hydrodenitrogenation. The measurements of H_2-D_2 exchange rate over bare and K-doped Mo_2C corroborated by DFT calculations revealed that the dissociative adsorption of hydrogen molecule, occurring on a single molybdenum site, is a nonactivated process, leading to the appearance of itinerant and highly reactive surface H atoms. They are slightly negatively charged with q_H varying from −0.152 to −0.176, depending on the position in the cluster. The experimentally determined barrier for H_2-D_2 exchange on Mo_2C was found to be 0.13 eV. Since hydrogen molecules readily dissociate and the resultant H atoms are mobile, the kinetic of the HDN reaction depends essentially on the rate of processes involving directly the indole molecule.

The HDN reaction of indole (IND), after its initial hydrogenation to indoline and C−N bond hydrogenolysis to orthoethylaniline (OEA), involves two routes. The first one (early denitrogenation route) starts from OEA, leading through dihydroaniline intermediate to ethylbenzene (EB) as a terminal product. The second one (late denitrogenation route) proceeds via hydrogenation of OEA to orthoethylcyclohexylamine and finally to ethylcyclohexane (ECH). These two pathways are additionally coupled by the transformation of EB into ECH

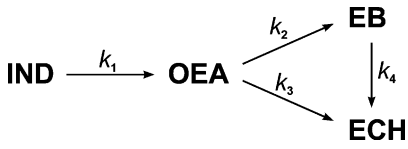

The kinetics (assuming the first-order Langmuir−Hinshelwood mechanism) of the whole process was modeled by adapting the parallel consecutive reaction network proposed in ref 31. Further details concerning the model and the derivation of the rate equations and determination of the corresponding rate constants for kinetically significant reaction steps can be found elsewhere.[47] Here, for the sake of further discussion, we inspect only the first step of indole decay due to its hydrogenation into the OEA intermediate. The rate of this process can be expressed as

$$r_{IND} = -\frac{d[IND]}{dt} = k_1[*IND][H*H][L^{-1}]$$

where H*H indicates surface hydrogen produced by dissociative adsorption of H_2(g) on a single active site (vide supra). Taking that the adsorption of indole and hydrogen are in quasiequilibrium and that at steady state conditions the number of unoc-

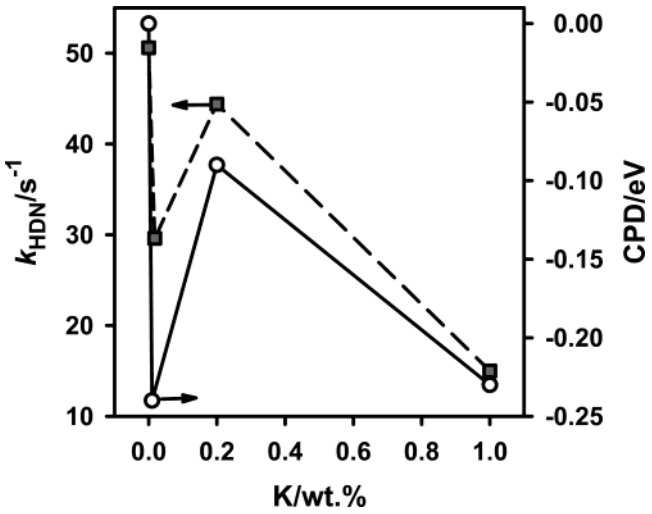

Figure 9. The dependence of the indole hydrodenitrogenation rate constant over K−Mo_2C and the work function of the catalyst as a function of potassium coverage.

cupied active sites [*] is small and nearly constant,[47] the above equation can be written as

$$r_{IND} = [*]^2 k_1 K_{H_2} p_{H_2} K_{IND} [L^{-1}][IND]$$

where K_{H_2} and K_{IND} stand for the corresponding hydrogen and indole adsorption equilibrium constants, respectively, and L is the density of the surface sites. This equation is to be compared to the global first-order rate law $r_{IND} = k_{IND}[IND]$.

The global rate constant k_{IND} of indole hydrogenation was derived from the nonlinear least-squares fit of the experimental data to the calculated kinetic curves using the Levenberg−Marquardt method. The R^2 coefficient of the fitting was better than 0.99, except of the sample with 1% of potassium, for which it dropped to 0.94. The k_{IND} values are collected in Table 1.

In Figure 9, the comparison of work function changes and the rate constant of HDN of indole as a function of potassium content in Mo_2C catalyst is presented. As can be noticed, both curves exhibit surprisingly similar K-dependence. At very low coverage, a sudden drop of k_{IND} is paralleled by the analogous sharp decrease in the contact potential difference. As the potassium loading increases, both parameters increase, passing through a local maximum at 0.2 wt % of K and then fall down in concert upon further K addition. It is probably worth mentioning here that an analogous, nonmonotonic correlation with potassium loading between the rate constant of DBT hydrogenation and the work function for the same catalyst was also noted.[48] These observations are in line with the previous investigations of the impact of alkali on small molecules adsorption on metal surfaces rationalized in terms of the energetic proximity of the Fermi level and molecular orbitals of adsorbing molecules.[9] The energy of the orbital with respect to the Fermi level determines the occupation of the orbital. It is particularly substantial for the electronic states near E_F. The interaction strength depends on the energy and filling of those orbitals, their bonding, and antibonding character, with the E_F being the most important determining parameter.[49]

The tight relationship between the k_{IND} and Φ implied that the electronic properties of the Mo_2C surface gauged by the position of the Fermi level is the primary factor controlling the rate of the indole hydrogenation (the first step in the HDN process). The interaction between the indole molecule and the Mo_2C surface at first approximation can be discussed in terms of the global reactivity descriptors.[50] Since the Mo_2C possesses metallic character (vide DOS structure in Figure 8) the Fermi level, E_F corresponds directly to the chemical potential μ of electrons. Thus, the electronegativities of the bare and doped catalysts, $\chi(Mo_2C) = 3.73$ eV and $\chi(K-Mo_2C) = 3.53$ eV, can be readily obtained from the relationship $\mu = -\chi$. Following Pearson,[45] the electronegativity of the indole molecule can be assessed from the energy of the frontier orbitals $\chi(\text{indole}) \cong -(E_{LUMO} + E_{HOMO})/2 = -(-0.243 - 5.68)/2 = 2.96$ eV. In a similar way, the chemical hardness of the indole molecule can be obtained, $\eta(\text{indole}) \cong E_{LUMO} - E_{HOMO} = 2.72$ eV, whereas for Mo_2C it is equal to zero because HOMO and LUMO energies obviously coalesce to the same E_F level. Since $\chi(\text{indole}) < \chi(\text{catalyst})$ the electron flow takes place from the indole toward the catalyst, which is tantamount with the electrophobic promotion.[9] The amount of charge transfer $\Delta\rho$ can be estimated by applying the electronegativity equalization principle[45]

$$\Delta\rho = \frac{\chi(\text{catalyst}) - \chi(\text{indole})}{2\eta(\text{indole})}$$

Substitution of numerical values for Mo_2C and K−Mo_2C gives $\Delta\rho = (3.73-2.96)/(2 \times 2.72) = 0.142$ and $(3.53-2.96)/(2 \times 2.72) = 0.105$, respectively. The withdrawal of electron density from indole takes place from a HOMO. This is the orbital of a'' symmetry, which in the pentagonal ring is responsible for the π-type bonding between C_2-C_3 atoms. The HDN process starts by the attack of the mobile hydrogen atoms at this fragment of the indole molecule. The depopulation of the HOMO weakens the C=C bond, and therefore the pentagonal ring becomes more prone for breaking apart, which constitutes the first step in the transformation of indole into orthoethylaniline.[51] The extent of the electron transfer to the catalyst depends on the position of the Fermi level, which is controlled by potassium coverage. Indeed, the rate constant k_{IND} of hydrodenitrogenation of indole over K−Mo_2C followed the changes in the work function of the catalyst (Figure 9).

The discussed local interactions of the indole molecule with the surface are complemented by a longer-range electrostatic interaction between the dipole moment of the indole molecule ($\mu(\text{indole}) = 2.7$ D) and the electric field created by the potassium adatom. The resultant nonuniform field at the surface perturbs the electron density in the indole molecule, affecting the orbital energies. This effect can be compared with the energy shift of the molecular orbitals of adsorbed reactants in the presence of strong external electric fields.[7]

While our results indicate that the E_F and DOS structure can be related to indole chemisorption and the rate of the resultant hydrogenation process (k_{IND}), it would not be correct to conclude that generally higher E_F leads to higher turnover. Clearly, the Fermi level of the catalyst should be in tune with the energy levels of indole for its influence on the activation to be effective. The results obtained here justify, however, further experimental and theoretical efforts to determine the boundaries of the validity of the simple semiqualitative frontier-orbital description developed in this paper. Obviously such picture should be complemented by a more accurate DFT modeling of the active ensemble composed of the Mo_2C cluster with adsorbed indole molecule surrounded by hydrogen which is now in progress.

4. Conclusions

The efficiency of electronic promotion gauged by the work function of the catalyst depends, in a nonmonotonic way, on the potassium parent solution and was greater for K/THF than

for KOH/2-propanol. The strongest effect was observed for low potassium loading ($\Theta_K < 0.02$), while further addition led to the agglomeration of the promoter, and the surface dipole responsible for work-function decrease is screened. The surface dipole moment ($\mu_S = 5.6$ D) and work-function decrease ($\Delta\Phi = 0.2$ eV) calculated from DFT modeling were in good agreement with the corresponding experimental data, analyzed in terms of the Helmholtz equation. The validity of the Schottky cycle for the work-function determination using desorption energies of potassium atoms and ions was confirmed by the independent CPD measurements. The changes in the catalyst work function with K addition show a remarkable correlation with the rate of catalytic hydrodenitrogenation of indole over Mo_2C.

Acknowledgment. This work was done within Research Project No. 3T09A17219, sponsored by the Polish Committee for Scientific Research.

References and Notes

(1) Boudart, M.; Levy, R. B. *Science* **1973**, *191*, 547.
(2) Schlatter, J. C.; Oyama, S. T.; Metcalf, J. E.; Lambert, J. M. *Ind. Eng. Chem. Res.* **1988**, *27*, 1648.
(3) Ramanathan, S.; Oyama, S. T. *J. Phys. Chem. B* **1995**, *99*, 16365.
(4) Chen, J. G. *Chem. Rev.* **1996**, *96*, 1479.
(5) Choi, J.-S.; Krafft, J.-M.; Krztoń, A.; Djéga-Mariadassou, G. *Catal. Lett.* **2002**, *81*, 175.
(6) Schwartz, V.; da Silva, V. T.; Oyama, S. T. *J. Mol. Catal. A* **2000**, *163*, 251.
(7) Mross, W. D. *Catal. Rev. Sci. Eng.* **1983**, *25*, 591.
(8) *Physics and Chemistry of Alkali Metal Adsorption*; Bonzel, H. P., Bradshaw, A. M., Ertl, G., Eds.; Elsevier: Amsterdam, 1989.
(9) *The Chemical Physics of Solid Surfaces, Coadsorption, Promoters and Poisons*; King, D. A., Woodruff, D. P., Eds.; Elsevier: Amsterdam, 1993; Vol. 6.
(10) Pacchioni, G.; Lomas, J. R.; Illas, F. *J. Mol. Catal.* **1997**, *119*, 263.
(11) Vayenas, C. G.; Brosda, S.; Pliangos, C. *J. Catal.* **2001**, *203*, 329.
(12) Zangwill, A. *Physics at Surfaces*; Cambridge University Press: New York, 1988; p 212.
(13) Thomas, J. M.; Thomas, W. J. *Principles and Practice of Heterogeneous Catalysis*; VCH: Weinheim, 1997.
(14) Hammer, B.; Norskov, J. K. *Adv. Catal.* **2000**, *45*, 71.
(15) Hoffman, R. In *Solids and Surfaces*; VCH: New York, 1988.
(16) Tong, Y. T.; Renouprez, A. J.; Martin, G. A.; Van der Klink, J. J. *Stud. Surf. Sci. Catal.* **1996**, *101*, 901.
(17) Feibelman, P.; Hamann, D. R. *Surf. Sci.* **1985**, *149*, 48.
(18) Bowker, M. In *Chemical Physics of Solid Surfaces*; King D. A., Woodruff, D. P., Eds.; Elsevier: Amsterdam, 1993; Vol. 6, Chapter 7.
(19) Volpe, L.; Boudart, M. *J. Solid State Chem.* **1985**, *59*, 348.
(20) Choi, J.-S.; Bugli, G.; Djéga-Mariadassou, G. *J. Catal.* **2000**, *193*, 238.
(21) Kojami, R.; Aika, K. *Appl. Catal. A: General* **2001**, *219*, 141.
(22) Kotarba, A.; Adamski, G.; Sojka, Z.; Witkowski, S.; Djega-Mariadassou, G. *Stud. Surf. Sci. Catal.* **2000**, *130*, 485.
(23) Engvall, K.; Holmlid, L.; Kotarba, A.; Pettersson, J. B. C.; Menon, P. G.; Skaugset, P. *Appl. Catal. A: General* **1996**, *134*, 239.
(24) Engvall, K.; Kotarba, A.; Holmlid, L. *J. Catal.* **1999**, *181*, 256.
(25) Vosko, S. H.; Wilk, L.; Nusair, M. *Can. J. Phys.* **1990**, *59*, 1200.
(26) Hermann, K.; Chakrabarti, A.; Haras, A.; Witko, M.; Tepper, B. *Phys. Status Solidi* **2001**, *187*, 137.
(27) Gomez-Balderas, R.; Oviedo-Roa, R.; Martinez-Magadan, J. M. *Surf. Sci.* **2002**, *518*, 163.
(28) Hugosson, H. W.; Eriksson, O.; Jansson, U.; Johansson, B. *Phys. Rev. B* **2001**, *63*, 134108.
(29) Schlegel, H. B. In *Ab initio Methods in Quantum Chemistry I*; Lawley, K. P., Ed.; Wiley: New York, 1987.
(30) Abe, H.; Bell, A. T. *Catal. Lett.* **1993**, *18*, 1.
(31) Miga, K.; Stańczyk, K.; Sayag, C.; Brodzki, D.; Djéga-Mariadassou, G. *J. Catal.* **1999**, *183*, 63.
(32) Wang, J.; Castonguay, M.; Den, J.; McBreen, P. H. *Surf. Sci.* **1997**, *374*, 197.
(33) Hagström, M.; Engvall, K.; Pettersson, J. B. C. *J. Phys. Chem. B* **2000**, *104*, 4457.
(34) Ozawa, K.; Anazawa, T.; Tokumitsu, S.; Sekine, R.; Miyazaki, E.; Edamoto, K.; Tanaka, S.; Otani, S. *Surf. Sci.* **1995**, *336*, 93.
(35) Papageorgopoulos, C. A.; Kamaratos, M.; Kennou, S.; Vlachos, D. *Surf. Sci.* **1991**, *251*, 1057.
(36) Vollmer, M.; Träger, F. *Surf. Sci.* **1987**, *187*, 445.
(37) Chalamala, B. R.; Wallace, R. W.; Gnade, B. E. *J. Vac. Sci. Technol. B* **1998**, *16*, 3073.
(38) Oyama S. T. *The Chemistry of Transition Metal Carbides and Nitrides;* Blackie Academic & Professional: Glasgow, 1996.
(39) Ionov, N. I. *Prog. Surf. Sci.* **1971**, *1*, 237.
(40) Mulle J. E. *The Chemical Physics of Solid Surfaces, Coadsorption, Promoters and Poisons*; King, D. A., Woodruff, D. P., Eds.; Elsevier: Amsterdam, 1993; Vol. 6, Chapter 2.
(41) Niemantsverdriet, J. W. *Spectroscopy in Catalysis*; VCH: Weinheim, 1993.
(42) Bredow, T.; Apra, E.; Catti, M.; Pacchioni, G. *Surf. Sci.* **1998**, *418*, 150.
(43) Hugosson, H. W.; Eriksson, O.; Jansson, U.; Johansson, B. *Phys. Rev. B* **2001**, *63*, 134108.
(44) Somorjai, G. A. *Introduction to Surface Chemistry and Catalysis*; Wiley: New York, 1994.
(45) Haber, J. *Catal. Sci Technol.* **1983**, *2*, 13.
(46) Haller, G. *J. Catal.* **2003,** *216*, 12.
(47) Adamski, G.; Dyrek, K.; Kotarba, A.; Sojka, Z.; Sayag, C.; Djéga-Mariadassou, G. *Catal. Today*. In press.
(48) Adamski, G.; Djéga-Mariadassou, G.; Dyrek, Sayag, C. K.; Kotarba, A.; Sojka, Z.; *Conference Abstracts*; Europacat-VI: Innsbruck, Austria; 31.08−4.09.2003, B3.108.
(49) Kolasinski K. W. *Surface Scence, Foundations of Catalysis and Nanoscience*; Wiley: New York, 2002.
(50) Pearson, R. G. *Chemical Hardness;* Wiley-VCH: Weinheim, 1997.
(51) Girgis, M. J.; Gates, B. C. *Ind. Eng. Chem. Res.* **1991**, *30*, 2021.